Chapter 6

Use of Synthetic and Natural Zeolites Tailored for As(V) Sorption

Andrey E. Krauklis

Additional information is available at the end of the chapter

http://dx.doi.org/10.5772/intechopen.72614

Abstract

Arsenic in drinking water poses serious potential health risks in more than 30 countries with total affected population of around 100 million people. Natural and synthetic zeolites can be tailored in order to obtain improved sorption of As(V) making them a relatively cheap and efficient material for water remediation. The chapter is concentrated on the zeolitic materials for water remediation, and reports new findings regarding modification methods and comparison of such materials for the use in As(V) sorption applications. Methods of modification of zeolites are developed and explained. On the experimental and novel scale, using developed methods, 11 novel materials are synthesized and studied. Initial and modified materials are characterized by optical microscopy, SEM and EDX, as well as by metal content in those which are determined using dissolution in acids and FAAS.

Keywords: zeolites, water remediation, As(V), adsorption, sorbents, arsenic, environmental remediation, equilibrium, kinetics, heavy metals, metalloids

1. Introduction

Groundwater contamination with arsenic compounds is an everyday problem for millions of people as water resources are crucial for use as drinking water, as well as in food production and agriculture [1–3]. Accumulation of arsenic in the body poses significant health risks and may lead to arsenicosis [3]. USA Environmental Protection Agency (EPA) in 2006 has diminished acceptable maximum contaminant level (MCL) for arsenic in drinking water from 50 down to 10 μg/L, and stricter norms have been set in headquarters of Peoples Republic of China, United Nations Health Organization, and European Union [4–6]. Arsenic contamination is both natural and due to anthropogenic sources. Weathering of rocks and minerals is a typical example of a natural process, while pesticides, metal waste, fertilizers and fossil fuel combustion are due to industrial and agricultural activities [7–9].

Sorption is considered as one of the most reasonable water remediation techniques because of its lower costs [10–13]. Zeolites are crystalline, microporous, hydrated aluminosilicate minerals containing alkali or alkaline cations. These materials are often praised for their efficient sorptive properties. Zeolite surface modification is a possible route for substantially improving oxyanion sorption [12]. Zeolites generally possess high values of specific surface area, which can be larger than 700 m^2/g [14]. This parameter is an extremely important one for adsorptive properties. Most of zeolitic water remediation technologies are based on cation exchange principles; however, there are cases when zeolites are used and useful for anion removal, such as cases of arsenate and arsenite sorption [15, 16]. Advantages of zeolitic sorbents are as follows: Generally, they are environmentally friendly, relatively cheap and can be treated for secondary use. Considering affinity of metalloids to interact with Fe and Mn-containing compounds [17], studies of As(V) sorption can be promoted in direction of using iron- and manganese-modified zeolites.

1.1. Clinoptilolite

Clinoptilolite is a high silicate content heulandite group mineral $(Na,K,Ca_{0.5},Sr_{0.5},Ba_{0.5},Mg_{0.5})_6[Al_6Si_{30}O_{72}]\ 20H_2O$ – HEU, often main component of natural zeolites. Its effective pore diameter is in range from about 4.5 up to 6.0 Å. Such clinoptilolite's properties as chemical stability in basic environments, thermostability and high sorption rate make it a useful material in chemical research and industry [15].

1.2. Zeolite A

Zeolite A is one of the most widely used synthetic zeolites. It has a Linde Type A (LTA) structural type as defined by International Zeolite Association (IZA). Most commonly used in its sodium form (4A), its chemical formula in dehydrated form is $[Na_{12}Al_{12}Si_{12}O_{48}]_8$ [18]. Potassium (3A) and calcium (5A) forms are also widely used. These zeolite names roughly represent pore opening diameters in ångstrøms (Å). It is possible to convert one form into another one via ion exchange [18].

1.3. Zeolite X

Zeolites X contain 12 rings or pore openings with a diameter of 7.4 Å (8.1 Å when completely empty). Diameter of the central cavity is 13.7 Å [19].

1.4. Iron oxides

Iron oxides and hydroxides are known for their use in wastewater treatment [20]. Natural iron oxides (without using zeolites as the host material) have affinity for arsenic compounds but show low sorption efficiency of treating aqueous solutions contaminated with As compounds (0.02–0.4 mg/g) due to low specific surface area [5, 21–23]. Thus it is important to introduce a host material with high specific surface area, i.e. zeolite, which can be modified with iron compounds, such as FeOOH. Fe(III) ionic radius is 0.67 Å [24], small enough in order to use it for modification of zeolites.

1.5. Manganese oxides

As(V) is sorbed more easily onto solid surfaces than As(III), and thus oxidation of As(III) followed by adsorption is a potentially effective route for the removal of arsenic compounds [25, 26]. It has been reported that clinoptilolite modification with MnO_2 significantly enhances sorption capacity of As(V) and is believed to be independent of pH [27]. MnO_2 can oxidize As (III) to As(V) based on sources [24, 28], which is backed up with the following red-ox reactions, shown in Eqs. 1 and 2:

$$HAsO_2 + 2H_2O \leftrightarrow H_3AsO_4 + 2H^+ + 2e^- \quad \left(\varphi^\circ = -0.56\ \mathrm{e}\right) \tag{1}$$

$$MnO_2 + 4H^+ + 2e^- \leftrightarrow Mn^{2+} + 2H_2O \quad \left(\varphi^\circ = +1.23\ \mathrm{e}\right) \tag{2}$$

The summary red-ox reaction is represented by Eq. 3:

$$HAsO_2 + MnO_2 + 2H^+ \leftrightarrow H_3AsO_4 + Mn^{2+} \quad \left(\varphi^\circ = +0.67\ \mathrm{e}\right) \tag{3}$$

The value of standard potential (ϕ° = +0.67 e) is positive, which indicates that equilibrium is shifted towards right of Eq. 3, in direction of As(V) as a product [24].

Mn(II), Mn(IV) and Mn(VII) ionic radii are 0.80–0.91 Å, 0.50–0.52 Å and 0.46 Å, respectively [24]. Mn-O bond in a permanganate ion is 1.629 Å, and Mn is in the tetrahedron's centre [29]. This is small enough in order to use it for modification of zeolites.

1.6. Sorption models

Langmuir and Freundlich isotherms are the most popular models in describing sorption in water environments; however, other models are also known and widely used such as Dubinin–Radushkevich, Temkin and Redlich–Peterson models [18, 30].

1.7. Langmuir model

The model is based on assumption that each sorption active centre is equivalent, and it is energetically irrelevant whether adjacent sorption centres are empty or already occupied [20]. Langmuir sorption model [31]:

$$q_e = \frac{q_m K_L C_e}{1 + K_L C_e}, \tag{4}$$

where q_e [mg/g] is equilibrium concentration in adsorbent which corresponds to initial concentration in solution C_0 [mg/L]; q_m [mg/g] is maximum monolayer coverage capacity; C_e [mg/L] is equilibrium concentration in solution; K_L [L/mg] is Langmuir constant.

Linearized form of Eq. 4 is represented with Eq. 5:

$$\frac{C_e}{q_e} = \frac{1}{q_m} C_e + \frac{1}{q_m K_L} \tag{5}$$

In order to compare experimental data's fit with the model, linearized form is used, plotting data in coordinates $\frac{C_e}{q_e}$ – C_e and obtaining determination coefficient R^2 [30].

1.8. Freundlich model

Freundlich model is based on assumption that sorption occurs on nonequivalent sorption centres, which is due to repulsion between the sorbed particles. It is assumed there is an infinite number of sorption centres [20]. Freundlich sorption model [32]:

$$q_e = K_F C_e^{\frac{1}{n}}, \tag{6}$$

where K_F [$mg^{1-1/n} \cdot L^{1/n}/g$] is Freundlich coefficient; n [−] is Freundlich constant.

Linearized form of Eq. 6 is represented with Eq. 7 [30]:

$$\ln q_e = \ln K_F + \frac{1}{n} \ln C_e \tag{7}$$

In order to compare experimental data's fit with the model, linearized form is used, plotting data in coordinates $\ln q_e$ – $\ln C_e$ and obtaining determination coefficient R^2 [30].

1.9. Dubinin-Radushkevich model

Usually the model is used to differentiate between physisorption and chemisorption. Initially it was used to describe physisorption. Dubinin-Radushkevich sorption model [33]:

$$q_e = q_s e^{\left(-K_{DR}\varepsilon_{DR}^2\right)} \tag{8}$$

$$\varepsilon_{DR} = RTln\left(1 + \frac{1}{C_e}\right) \tag{9}$$

$$E = \frac{1}{\sqrt{2K_{DR}}}, \tag{10}$$

where ε_{DR} [kJ/mol] is Dubinin–Radushkevich isotherm variable; E [kJ/mol] is mean free energy of adsorption; q_s [mg/g] is theoretical Dubinin–Radushkevich saturation sorption capacity; K_{DR} [mol^2/kJ^2] is Dubinin–Radushkevich constant.

Linearized form of Eq. 8 is represented with Eq. 11 [30]:

$$\ln q_e = \ln q_s - K_{DR}\varepsilon_{DR}^2 \tag{11}$$

In order to compare experimental data's fit with the model, linearized form is used, plotting data in coordinates $\ln q_e$ – ε_{DR}^2 and obtaining determination coefficient R^2 [30].

1.10. Temkin model

The model is based on assumption that heat of adsorption (function of temperature) decreases linearly with increasing amount of sorbed particles. Temkin sorption model [33]:

$$q_e = \frac{RT}{b_T} \ln K_T C_e, \tag{12}$$

where R [8.314 J/(mol·K)] is universal gas constant; T [K] is temperature; K_T [mg/L] and b_T $\left[\frac{J \cdot g}{mol \cdot L}\right]$ are parameters describing adsorbate-adsorbent interactions.

Linearized form of Eq. 12 is represented with Eq. 13 [30]:

$$q_e = \frac{RT}{b_T} \ln K_T + \frac{RT}{b_T} \ln C_e \tag{13}$$

In order to compare experimental data's fit with the model, linearized form is used, plotting data in coordinates q_e – lnC_e and obtaining determination coefficient R^2 [30].

1.11. Redlich-Peterson model

The model is a hybrid between Langmuir and Freundlich models. When value of coefficient β_{RP} is equal to 1, the model becomes equivalent with Langmuir model. Often this three-parameter model is able to explain experimental data more precisely. Redlich–Peterson sorption model [34]:

$$q_e = \frac{K_{RP} C_e}{1 + \alpha_{RP} C_e^{\beta_{RP}}}, \tag{14}$$

where α_{RP} $\left[\left(\frac{L}{mg}\right)^{\frac{1}{\beta_{RP}}}\right]$, β_{RP} [−] and K_{RP} [L/g] are Redlich–Peterson isotherm parameters.

Linearized form of Eq. 14 is represented with Eq. 15 [30, 34]:

$$\ln\left(K_{RP}\frac{C_e}{q_e} - 1\right) = \beta_{RP} \ln C_e + \ln \alpha_{RP} \tag{15}$$

K_{RP} is optimized by finding the closest fit to the model via the highest determination coefficient. In order to compare experimental data's fit with the model, linearized form is used, plotting data in coordinates $\ln\left(K_{RP}\frac{C_e}{q_e} - 1\right)$ – $\ln C_e$ and obtaining determination coefficient R^2 [30, 34].

1.12. Purpose and aim of this work

The purpose of this work is to present zeolites as potential sorbents for As(V) sorption for water remediation as well as to present novel modification methods and materials. The aim of the study is to provide and interpret results of As(V) sorption onto raw and modified zeolites.

2. Materials

2.1. Slovakian natural clinoptilolite (Slov)

Clinoptilolite natural zeolite from Slovakian deposit Nižný Hrabovec was used. Its specific weight is 2200–2440 kg/m^3; porosity 24–32%; clinoptilolitic content fluctuates in range from 86

to 94%; according to manufacturer, it also contains cristobalite, clay mica, plagioclase, rutile, quartz; Si:Al ratio is in range 4.80–5.40; fraction of 1–2.5 mm was used [35].

2.2. Ukrainian natural clinoptilolite (Ukr)

Clinoptilolite natural zeolite from Ukrainian Zakarpattian deposit Sokirnicke (ukr. Сокирницьке родовище). Specific weight 2370 kg/m^3; porosity 44%; clinoptilolitic content 77%; fraction 1–3 mm [36].

2.3. Russian natural clinoptilolite (Khol)

Clinoptilolite natural zeolite from Russian Zabaykalsky Krai deposit Kholinskoe (rus. Холинское месторождение). Specific weight 1900–2800 kg/m^3, bulk density 1.02–1.20 g/cm^3. Porosity is in range of 20–23% [37]. Zeolite was crushed and sieved using vibro sieve FRITSCH analysette 3 SPARTAN (Germany; International), collecting fraction from 0.8 up to 1.4 mm.

2.4. Synthetic zeolite A (4A)

SYLOSIV A 4 was used (purchased from Grace Davison, USA), zeolite 4A in fine powder form (particle size 6–9 μm). According to manufacturer, this material is chemically stable in basic, neutral and weak acidic environments; specific surface area 800 m^2/g; effective pore volume 0.25–0.30 cm^3/g; specific weight 1900–2300 kg/m^3 [38].

2.5. Synthetic zeolite X (13X)

Zeolite 13X was used (purchased from Hong Kong Chemical Corp.). Bulk density 0.601 g/cm^3; porosity 0.55%; fraction 4–5 mm.

2.6. Reagents

All compounds used were of analytical grade (≥ 98%) and were used without further purification. Sodium hydroxide, potassium chloride and 65% nitric acid were obtained from Sigma-Aldrich (Riedel-de Haën, Germany). Iron(III) chloride hexahydrate, calcium chloride dihydrate and 30% hydrogen peroxide were obtained from Enola (Riga, Latvia). Manganese(II) chloride tetrahydrate was obtained from Firma Chempur (Piekary Śląskie, Poland). All aqueous solutions were prepared using high purity deionized water (10–15 MΩ·cm), produced via water purification system Millipore Elix 3 (Billerica, USA). Arsenate stock solution was prepared using disodium hydrogenarsenate heptahydrate $Na_2HAsO_4{\cdot}7H_2O$ obtained from Alfa Aesar (Haverhill, USA).

3. Zeolite modification methods

Zeolites Ukr, Slov, Khol, 4A and 13X were modified using 6 different methods. Altogether, using these methods, 11 novel materials were synthesized and are described in this chapter. Additionally, FeOOH-modified zeolites A were obtained and described in the following source [17]. It should be also noted that another aluminosilicate, clay montmorillonite was modified using a similar approach and described in another work [39].

3.1. First method

First method is based on the method described in source [40]. The basis for FeOOH-modified sorbent synthesis is the iron oxohydroxide precipitation on the raw material. Description of modification is the following: 0.25 mol $FeCl_3 \cdot 6H_2O$ is dissolved in 250 mL DI water, adding 250 mL 3 M NaOH solution and aged for 3 h. Obtained $Fe(OH)_3$ precipitates are decanted. 100 g of raw material are mixed in the $Fe(OH)_3$ dispersion. The mixture is then carefully mixed and filtered under vacuum and washed with 250 mL DI water. The filtered and washed material is then dried in air atmosphere for 1 h at room temperature and then dried in the oven Gallenkamp Plus II (London, UK) for 4 h at 60°C.

Materials obtained using this method: Fe-Ukr(1); Fe-Slov.

3.2. Second method

Second method is based on the first method, modified based on the idea that the material is first soaked with a respective metal salt, followed by the reaction (FeOOH synthesis) inside the zeolite structure. The developed method is the following: 1 M $FeCl_3 \cdot 6H_2O$ solution is prepared and 100 g of zeolite are placed into it. The mixture is aged for 24 h. The mixture is then filtered, and without washing, 250 mL of 3 M NaOH solution are added to the soaked material and aged for 24 h. The mixture is filtered under vacuum and washed with 250 mL DI water. The filtered and washed material is dried in air atmosphere for 1 h at room temperature and subsequently dried in the oven Gallenkamp Plus II (London, UK) for 4 h at 60°C.

Materials obtained using this method: Fe-Ukr(2); Fe-13X; Fe-KHol.

3.3. Third method

Third method is based on the first method, adapted to be applicable for efficient modification of powders (as in case of Fe-4A and Fe-5A described in another work [17]). The idea is to conduct a reaction in the wet FeOOH mass, simplifying and accelerating modification process. The developed method is the following: 0.25 mol $FeCl_3 \cdot 6H_2O$ is dissolved in 250 mL DI water, 250 mL of 3 M NaOH is added and the mixture is aged for at least 3 h. Synthesized $Fe(OH)_3$ precipitates are decanted. The mass is filtered under vacuum, mixing in 100 g of raw material into the $Fe(OH)_3$ precipitates, while carefully mixing. Porridge-consistency mixture is washed with 250 mL DI water. The filtered and washed material is then dried in air atmosphere for 2 h at room temperature, and further dried in the oven Gallenkamp Plus II (London, UK) for 4 h at 110°C.

Materials obtained using this method: Fe-Ukr(3); in combination with other methods, FeMn-Slov with fourth method.

3.4. Fourth method

Fourth method is based on methods described in sources [27, 41] which are natural zeolite modification methods with manganese oxides. Concentrations used are the same as described in source [27]. 100 g of zeolite is weighted in the beaker and dried in air atmosphere from initial moisture in air atmosphere in the oven for 1 h at 70°C. 2.5 M $MnCl_2$ solution and 10 M NaOH solution are prepared. 100 mL of prepared 2.5 M $MnCl_2$ solution is added, while

mixing, to the zeolite in the beaker. 1 mL of prepared 10 M NaOH solution is added and mixed. Solution is aged for 24 h. Without filtering, the mixture is placed in the oven for 3 h at 150°C. The result is densified zeolite granule/pellet mass, covered with precipitates. This mass is then placed into the crucibles. Crucibles with the obtained mass are placed in the muffle furnace and are held there for 5 h in air atmosphere at 550°C. Crucibles are then taken out and cooled down in air at room temperature. After cooling, modified zeolite is washed with 300 mL of DI water. Material is dried in air for 1 h at room temperature, and further dried in the oven Gallenkamp Plus II (London, UK) for 4 h at 60°C.

Materials obtained using this method: Mn-Slov(1); in combination with other methods, FeMn-Slov with third method, CaMn-Slov with sixth method.

3.5. Fifth method

Fifth method is based on fourth method, but, while fourth method is rooted in Mn(II) oxidation at elevated temperature, this method is based on Mn(VII) reduction reaction using ethanol. The reaction as represented by Eq. 16 is conducted at room temperature [42]:

$$2KMnO_4 + 3C_2H_5OH \rightarrow 2MnO_2 + 3CH_3CHO + 2KOH + 2H_2O \quad (16)$$

This modification method is developed and chosen in order to perform modification of zeolites with MnO_2 in softer conditions at room temperature. Concentration and volume of potassium permanganate solution is chosen based on $KMnO_4$ solubility in water at room temperature (if limited by) and in order to introduce the same amount of Mn atoms as in fourth method (0.25 mol Mn). The amount of ethanol is chosen such so that C_2H_5OH and $KMnO_4$ are in molar ratio 1:1 (stoichiometrically). 100 g of zeolite is weighted in the beaker. Then, 1.5 L 0.17 M $KMnO_4$ solution is prepared and added into the beaker with the zeolite. The aging proceeds for 96 h in the solution. Then, 24.3 mL 60% C_2H_5OH is added to the mixture in order to reduce $KMnO_4$. Acetaldehyde is obtained and characteristic smell can be felt. Modified zeolite is filtered under vacuum and washed with 300 mL DI water. Material is then dried in air atmosphere at room temperature for 1 h, and further dried in the oven Gallenkamp Plus II (London, UK) for 4 h at 60°C.

Materials obtained using this method: Mn-Slov(2), Mn-4A.

3.6. Sixth method

The sixth method is a Ca^{2+} ion-exchange reaction used in combination with previously described methods. It is based on a principle that one can tailor the effective micropore diameter in zeolites by exchanging the cations. Divalent Ca^{2+} cations are used to increase the effective pore opening [18]. 20 g of zeolite are placed in 100 mL glass vessels. 4.5 M $CaCl_2$ solution is prepared and 50 mL is added to the material. The vessels are then placed on the orbital shaker Biosan Multi-functional Orbital Shaker PSU-20i (Riga Latvia), setting frequency to 150 rpm for 96 h. The mass is decanted and then washed with 100 mL DI water. Afterward, the material is dried for 2 h at room temperature in air atmosphere, and then subsequently dried at 110°C in the oven for 4 h.

Materials obtained using this method: in combination with other methods, CaMn-Slov with fourth method.

4. Material characterization

Modified and raw zeolites were characterized using optical microscopy, scanning electron microscopy (SEM), energy-dispersive X-ray spectroscopy (EDX, EDS), by analysis of Fe and Mn content, which was performed by dissolution in acids followed by flame atomic absorption spectrometry (FAAS). Bulk density of all sorbents was determined.

4.1. Optical microscopy

Optical microscopy allows to study the surface of the material and to evaluate homogeneity. Optical microscope Leica was used with a digital camera Leica DFC480, ocular Leica 10X/21B, which enables magnification from x7.1 up to x115. Additional lighting was used: Leica Fluorescent Ringlight and Leica CLS150X (Germany; International) [43]. Software used for obtaining images was Leica Application Suite v4.1.0. A square of 1 cm was cut out of millimetre paper, which was placed adjacent to the sample as a scale. In order to obtain qualitative images, 11 micrographs were used on average using focus stacking (pyramid) approach. Software used for stacking was Helicon Focus (Kharkiv, Ukraine).

4.2. SEM and EDX

Materials were covered with a thin layer of gold in order to prevent charging due to electron beam. Gold sputtering was performed using Quorum Technologies Emitech K550X (Laughton, UK). Methods were performed using Tescan Mira/LMU (Brno, Czech Republic) in backscattered electron regime with working voltage of 15 kV.

4.3. FAAS

Fe and Mn content was obtained using dissolution in acids followed by flame atomic absorption spectrometry (FAAS). 1 g of each material was weighed in a beaker, using analytical scales (± 0.1 mg). 25 mL 65% HNO_3 and 5 mL 35% H_2O_2 were then added in each beaker. Beakers were placed in a thermostat Biosan MyLab Thermo-Block TDB 400 (Riga, Latvia) and heated up to 160°C. When half of the solution had evaporated, 25 ml 65% HNO_3 was added while heating the sample. The solutions were allowed to cool down in air at room temperature, filtered into a graduated vessel and diluted with DI water to a total volume of 60 mL each. Furthermore, a blank sample was prepared for background correction. 10 mL of each solution were moved in test tubes, using pipettes. Prepared samples were analysed using PerkinElmer AAnalyst 200 (Waltham, USA) with flame atomization. Mn and Fe content measurements were performed using background correction in air–acetylene flame. Fe and Mn content in samples was calculated using Eqs. 17 and 18:

$$w_{Fe} = C_{Fe} \cdot \frac{V}{m} \tag{17}$$

$$w_{Mn} = C_{Mn} \cdot \frac{V}{m}, \tag{18}$$

where w_{Fe} and w_{Mn} are Fe and Mn mass fractions in materials, respectively [mas%]; C_{Fe} and C_{Mn} are Fe and Mn ion concentartions in solution, respectively [mg/L]; V is volume of the solution (0.060 L) [L]; m is mass of sorbent (1000 mg) [mg].

4.4. Determination of bulk density

The method of bulk density determination is based on a standard method, which is described in literature [44–46]. An empty 250 mL graduated cylinder was weighted, using analytical scales Kern ALJ 220–4 (± 0.1 mg). Approximately, 100 g of powder or granules/pellets were placed in the graduated cylinder, while determining the total mass of material and the cylinder. Deducing cylinder's mass from the total, the mass of the material was obtained. The cylinder was gently hit on the flat surface until the material became compacted and the change in volume was not observable. The volume of the material was determined using the closest mark on the graduated cylinder. The bulk density was determined as the ratio of obtained mass and volume.

5. Sorption experiments

Sorption experiments were conducted using batch system. $Na_2HAsO_4{\cdot}7H_2O$ was used for preparing arsenic stock solutions at various concentrations (300, 200, 100, 50, 25, 10 and 5 mg/L). 0.5000 ± 0.0001 g of each sorbent was weighed in every 100 mL glass vessel using analytical scales Kern ALJ 220–4 (Balingen, Germany). 30.00 ± 0.05 mL of an As(V) solution was then added to every vessel with the adsorbent. Vessels were then shaken for 24 h at room temperature (23 ± 1°C) at 150 rpm using orbital shaker Biosan Multi-functional Orbital Shaker PSU-20i (Riga, Latvia) to ensure sorption equilibrium was achieved. Suspensions were filtered into 50 mL test tubes, and concentration of As(V) in the filtrate was then analysed using PerkinElmer AAnalyst 200 with flame atomization. Absorption was measured using background correction in N_2O-C_2H_2 flame. A spectral line of 193.7 nm was used. FAAS spectrometer was calibrated with 1000 mg As/L standard solutions obtained from Scharlau (Barcelona, Spain) (As_2O_3 in 0.5 M HNO_3). Each measurement was performed 3 times. In order to ensure arsenic analysis quality control, experiments were performed systematically; accurate As(V) concentration of respective stock solutions was measured 3 times and standard deviation was determined, which then was taken into account when describing sorption capacity of the materials.

6. Experimental results

6.1. Homogeneity and bulk density

Homogeneity of materials was evaluated using optical microscope. All studied materials were homogeneous except Fe-Ukr(1), Fe-Ukr(2), Fe-Ukr(3) and Fe-Slov. Due to inhomogeneities, these materials were not further analysed with SEM and EDX. Obtained information about bulk density and homogeneity is summarized in **Table 1**.

6.2. Metal ion content

Fe and Mn content by weight in all materials is summarized in **Table 2** as an average of three repeated measurements with standard deviation. Material with highest Fe content is FeMn-Slov

Material	Bulk density ($\frac{g}{mL}$)	Form	Homogeneity
4A	0.46 ± 0.02	Powder	Homogeneous
Mn-4A	0.77 ± 0.03	Powder	Homogeneous
13X	0.75 ± 0.03	Granules/Pellets	Homogeneous
Fe-13X	0.74 ± 0.03	Granules/Pellets	Homogeneous
Ukr	1.04 ± 0.04	Granules/Pellets	Homogeneous
Fe-Ukr(1)	1.05 ± 0.04	Granules/Pellets	Non-homogeneous
Fe-Ukr(2)	1.01 ± 0.04	Granules/Pellets	Non-homogeneous
Fe-Ukr(3)	1.00 ± 0.04	Granules/Pellets	Non-homogeneous
Slov	0.91 ± 0.04	Granules/Pellets	Homogeneous
Fe-Slov	0.92 ± 0.04	Granules/Pellets	Non-homogeneous
Mn-Slov(1)	1.12 ± 0.04	Granules/Pellets	Homogeneous
Mn-Slov(2)	0.97 ± 0.04	Granules/Pellets	Homogeneous
FeMn-Slov	0.91 ± 0.04	Granules/Pellets	Homogeneous
CaMn-Slov	1.11 ± 0.04	Granules/Pellets	Homogeneous
Khol	0.90 ± 0.04	Granules/Pellets	Homogeneous
Fe-Khol	0.96 ± 0.04	Granules/Pellets	Homogeneous

Table 1. Material bulk density, form and homogeneity.

Material	Fe content (mas%)	Mn content (mas%)
4A	0.19 ± 0.01	0.00 ± 0.01
Mn-4A	0.03 ± 0.00	0.57 ± 0.02
13X	0.34 ± 0.01	0.01 ± 0.01
Fe-13X	2.92 ± 0.11	0.02 ± 0.00
Ukr	0.53 ± 0.02	0.01 ± 0.01
Fe-Ukr(1)	1.37 ± 0.05	0.02 ± 0.01
Fe-Ukr(2)	1.67 ± 0.06	0.01 ± 0.01
Fe-Ukr(3)	1.70 ± 0.06	0.05 ± 0.01
Slov	0.45 ± 0.02	0.01 ± 0.01
Fe-Slov	8.75 ± 0.33	0.05 ± 0.01
Mn-Slov(1)	0.47 ± 0.02	4.58 ± 0.17
Mn-Slov(2)	0.43 ± 0.02	0.33 ± 0.01
FeMn-Slov	19.22 ± 0.73	2.80 ± 0.10
CaMn-Slov	0.35 ± 0.01	3.68 ± 0.13
Khol	0.33 ± 0.01	0.03 ± 0.01
Fe-Khol	1.43 ± 0.05	0.06 ± 0.01

Table 2. Fe and Mn content of materials obtained using FAAS.

(19.22 ± 0.73 mas%). Materials with highest Mn content are Mn-Slov(1) (4.58 ± 0.17 mas%), CaMn-Slov (3.68 ± 0.13 mas%) and FeMn-Slov (2.80 ± 0.10 mas%).

6.3. Optical microscopy

All raw and modified materials were studied using optical microscopy. Optical micrographs were obtained at different magnifications: x7.1, x20 and x80; and x115 for some materials. Optical micrographs with magnification of x80 for all studied materials are summarized in **Figure 1**.

Optical micrographs (**Figure 1**) indicate that obtained materials FeMn-Slov, Fe-Khol, Fe-13X, Fe-Ukr(1), Fe-Ukr(2), Fe-Ukr(3) and Fe-Slov are modified with an iron compound. Furthermore, also in x80 magnification materials look homogeneous, except Fe-Ukr(1), Fe-Ukr(2), Fe-Ukr(3) and Fe-Slov, where iron compound covers only parts of the materials' surface. Optical micrographs (**Figure 1**) also indicate that obtained materials Mn-4A, Mn-Slov(1), Mn-Slov(2), FeMn-Slov and CaMn-Slov are modified with manganese compounds.

6.4. Scanning electron microscopy

All raw and modified materials, except for nonhomogeneous Fe-Ukr(1), Fe-Ukr(2), Fe-Ukr(3) and Fe-Slov are studied with scanning electron microscopy (SEM). SEM micrographs are summarized in **Figure 2**.

SEM micrographs (**Figure 2**) indicate that obtained materials FeMn-Slov, Fe-Khol and Fe-13X are modified with an amorphous compound, which is also further proved using EDX (for more details, also see source [17]). SEM micrographs (**Figure 2**) indicate that obtained materials Mn-4A, Mn-Slov(1), Mn-Slov(2), FeMn-Slov and CaMn-Slov are modified with manganese compounds. In case of Mn-4A and Mn-Slov(2), manganese compound is amorphous, while for Mn-Slov(1), FeMn-Slov and CaMn-Slov a new crystalline phase ($Mn_8O_{10}Cl_3$) is obtained (more details can be found in source [17]).

6.5. Energy-dispersive X-ray spectroscopy

All raw and modified materials, except nonhomogeneous Fe-Ukr(1), Fe-Ukr(2), Fe-Ukr(3) and Fe-Slov were studied with energy-dispersive X-ray spectroscopy (EDX). EDX results are summarized in **Table 3**. Elements with probability ≥95% are shown as an average of 6 repeated measurements at different locations.

Analysing amorphous iron compounds with EDX, it was deduced that it consists of 65.28 ± 3.91 mas% Fe and 34.72 ± 2.08 mas% O. This result is in agreement with elemental content of FeOOH (62.85 mas% Fe, 36.01 mas% O and 1.14 mas% H).

Analysing manganese crystals with EDX, it was deduced that it consists of 54.58 ± 3.27 mas % Mn, 30.27 ± 1.82 mas% O and 15.15 ± 0.91 mas% Cl. This result is in agreement with elemental content of $Mn_8O_{10}Cl_3$ (62.26 mas% Mn, 22.67 mas% O, 15.07 mas% Cl). Elevated oxygen content can be explained with signal from zeolite oxygen and/or with other manganese oxide presence.

http://dx.doi.org/10.5772/intechopen.72614

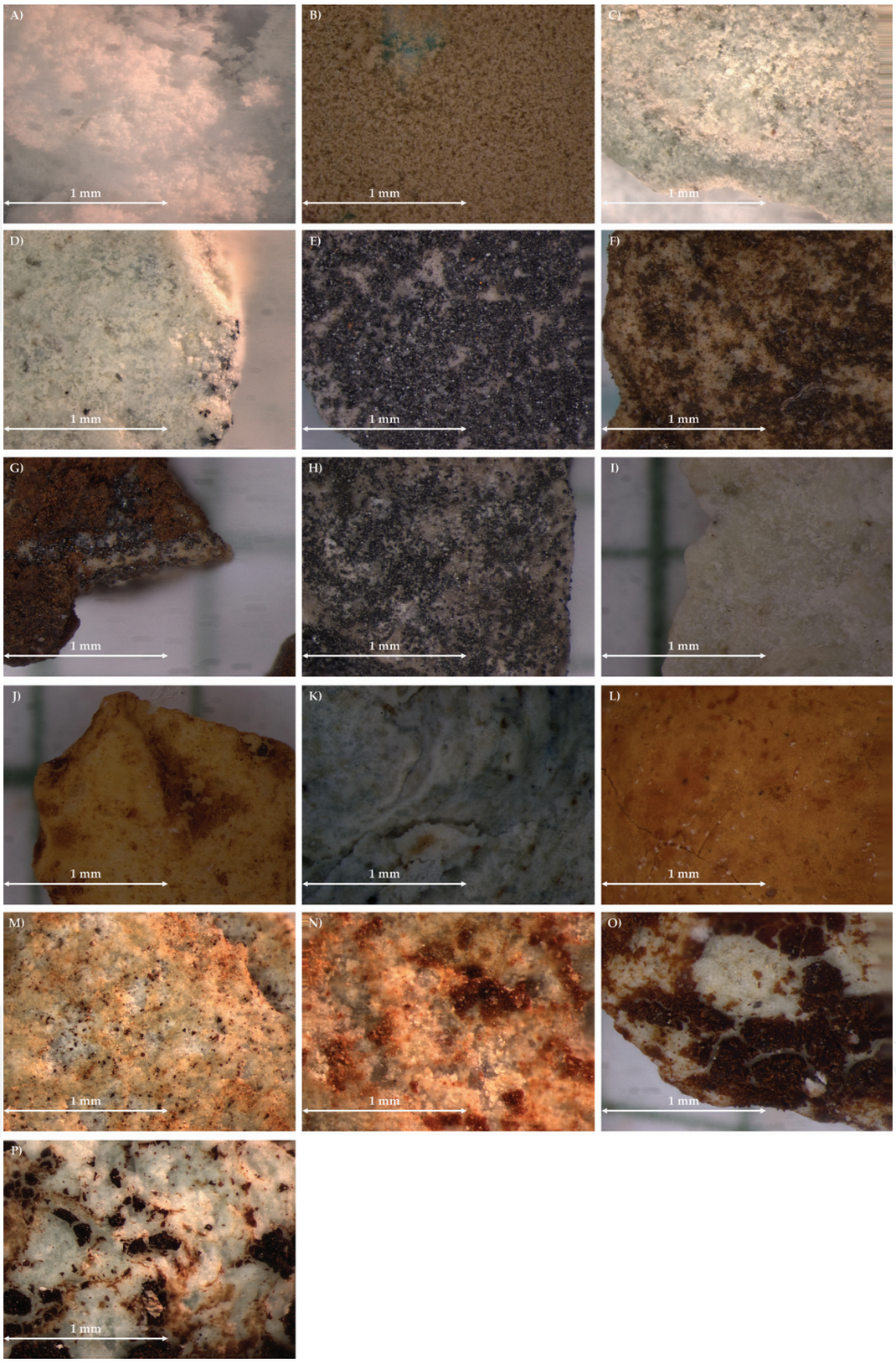

Figure 1. Optical micrographs with x80 magnification of all studied materials: (A) 4A; (B) Mn-4A; (C) Ukr; (D) Slov; (E) Mn-Slov(1); (F) Mn-Slov(2); (G) FeMn-Slov; (H) CaMn-Slov; (I) Khol; (J) Fe-Khol; (K) 13X; (L) Fe-13X; (M) Fe-Ukr(1); (N) Fe-Ukr(2); (O) Fe-Ukr(3); (P) Fe-Slov.

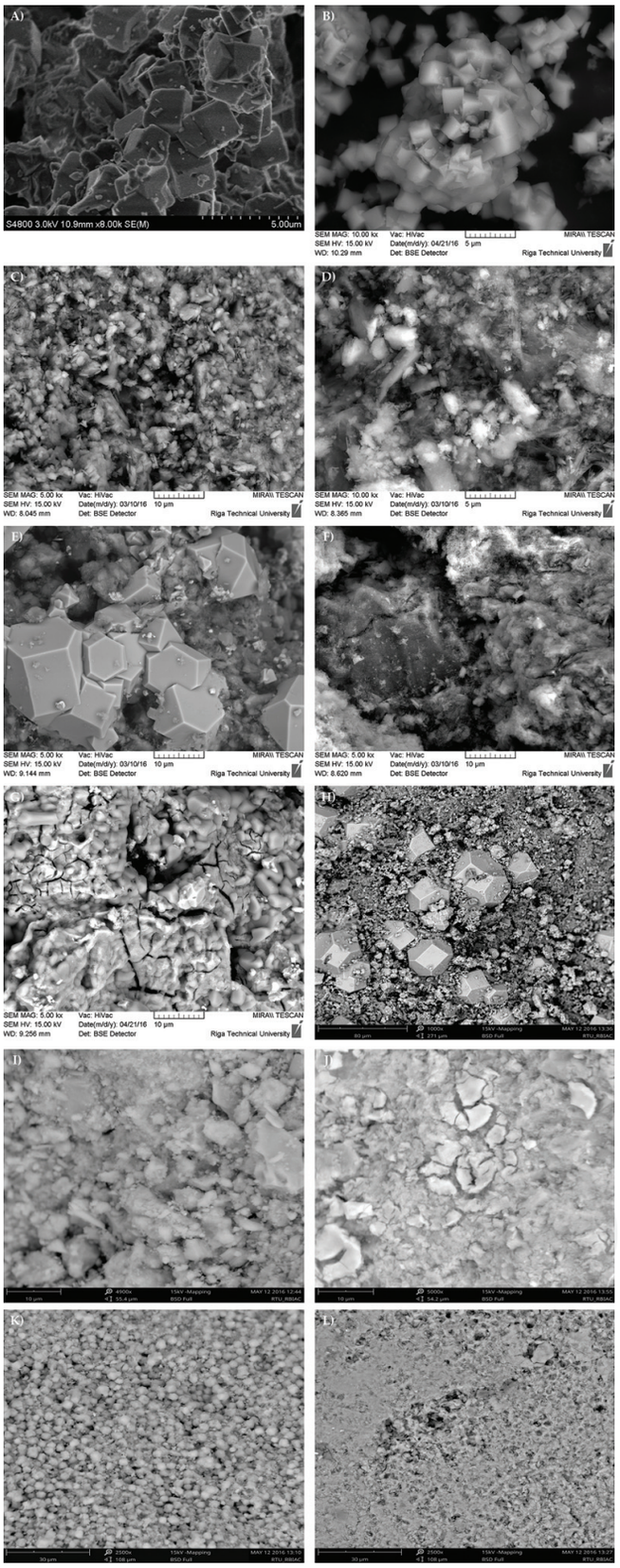

Figure 2. SEM micrographs of studied materials: (A) 4A; (B) Mn-4A; (C) Ukr; (D) Slov; (E) Mn-Slov(1); (F) Mn-Slov(2); (G) FeMn-Slov; (H) CaMn-Slov; (I) Khol; (J) Fe-Khol; (K) 13X; (L) Fe-13X.

Material	Elemental content [mas%]							
	Al	**Si**	**O**	**Fe**	**Mn**	**Cl**	**Na**	**Ca**
4A	14.76 ± 0.91	15.71 ± 0.95	55.59 ± 1.89	—	—	—	13.94 ± 0.53	—
Mn-4A	19.90 ± 1.22	20.62 ± 1.26	46.55 ± 2.85	—	1.74 ± 0.11	—	11.19 ± 0.68	—
Ukr	6.43 ± 0.39	35.94 ± 2.20	52.10 ± 3.19	2.80 ± 0.17	—	—	—	2.74 ± 0.17
Slov	5.27 ± 0.32	31.70 ± 1.94	59.94 ± 3.67	1.50 ± 0.09	—	—	—	1.58 ± 0.10
Mn-Slov(1)	3.86 ± 0.24	31.66 ± 1.94	47.33 ± 2.90	0.71 ± 0.04	8.40 ± 0.51	5.97 ± 0.37	0.24 ± 0.01	1.83 ± 0.11
Mn-Slov(2)	4.05 ± 0.25	22.51 ± 1.38	59.66 ± 3.65	1.37 ± 0.08	10.64 ± 0.65	—	—	1.76 ± 0.11
FeMn-Slov	3.16 ± 0.17	19.38 ± 1.05	43.28 ± 2.34	6.31 ± 0.34	11.10 ± 0.60	6.15 ± 1.04	9.24 ± 0.50	1.38 ± 0.07
CaMn-Slov	3.48 ± 0.22	24.69 ± 1.51	48.37 ± 3.06	1.80 ± 0.11	7.86 ± 0.48	7.41 ± 0.45	—	6.40 ± 0.39
Khol	8.96 ± 0.55	36.15 ± 2.21	51.25 ± 3.14	2.50 ± 0.15	—	—	0.42 ± 0.03	0.73 ± 0.04
Fe-Khol	5.20 ± 0.31	17.43 ± 1.05	64.08 ± 3.80	7.38 ± 0.57	—	1.53 ± 0.09	4.28 ± 0.26	0.10 ± 0.01
13X	14.56 ± 0.89	22.97 ± 1.41	52.15 ± 3.19	1.95 ± 0.12	—	—	7.95 ± 0.48	0.41 ± 0.03
Fe-13X	16.67 ± 1.02	23.59 ± 1.44	51.00 ± 3.12	5.62 ± 0.34	—	—	2.91 ± 0.18	0.20 ± 0.01

Table 3. EDX results (elements with probability ≥95%).

6.6. As(V) sorption experiments

Experimental data is compared with sorption models: Langmuir, Freundlich, Dubinin–Radushkevich, Temkin and Redlich–Peterson isotherm linearized forms comparing obtained determination coefficients (R^2). As(V) sorption experimental results and determination coefficients of fit with the sorption models are reported in **Table 4**.

As(V) sorption on raw zeolites is most precisely characterized by Freundlich's sorption model in all cases. As(V) sorption on iron oxohydroxides indicates that for these materials physisorption is dominant [3]. As(V) on Fe(III)-modified clinoptilolite and synthetic zeolites is most precisely characterized by Langmuir model [17, 20], which is also consistent with experimental data in this work, except for Fe-Ukr(2). Inconsistency in case of Fe-Ukr(2) can be explained by material's inhomogeneity, leaving large areas of zeolite unmodified.

As(V) sorption on Mn-modified zeolites is most precisely characterized with Freundlich model in cases of Mn-Slov(1), FeMn-Slov and CaMn-Slov and with Redlich–Peterson model in cases of Mn-4A and Mn-Slov(2).

Obtained As(V) equilibrium sorption capacities and Langmuir monolayer coverage (where applicable) are systematized in **Table 5**. Improvement shows how much material's equilibrium sorption capacity (at the highest studied As(V) solution concentration of 300 mg As(V)/L) increased after modification. Each sorption experiment was performed 3 times and obtained results represent average with standard deviation.

As(V) sorption isotherms for each respective material group (raw and modified, from top to bottom: Slov, Ukr, Khol, A and X) are shown in **Figure 3**.

Material	Determination coefficient R^2				
	Langmuir	**Freundlich**	**Dubinin–Radushkevich**	**Temkin**	**Redlich–Peterson**
4A	0.0586	**0.8401**	0.2180	0.7655	0.3729
Mn-4A	0.9911	0.9935	0.5360	0.9629	**0.9990**
Ukr	0.3874	**0.9724**	0.4559	0.7704	0.7768
Fe-Ukr(1)	**0.9853**	0.8693	0.6305	0.8840	0.9342
Fe-Ukr(2)	0.9062	**0.9872**	0.6655	0.8849	0.9635
Fe-Ukr(3)	**0.9990**	0.9342	0.8974	0.9452	0.9875
Slov	0.7607	**0.9801**	0.4944	0.8226	0.9314
Fe-Slov	**0.9936**	0.9299	0.8849	0.9404	0.8459
Mn-Slov(1)	0.9896	**0.9932**	0.6416	0.8834	0.7678
Mn-Slov(2)	0.9625	0.9838	0.4748	0.9015	**0.9938**
FeMn-Slov	0.9704	**0.9722**	0.7660	0.9174	0.3561
CaMn-Slov	0.5771	**0.9750**	0.5346	0.6840	0.8770
KHol	0.6213	**0.9379**	0.3429	0.7111	0.8379
Fe-KHol	**0.9968**	0.8968	0.9726	0.9599	0.8998
13X	0.5236	**0.9610**	0.5364	0.7113	0.6179
Fe-13X	0.7705	**0.9720**	0.4454	0.8207	0.9271

Table 4. As(V) sorption data and comparison with sorption models. Values marked in bold signify a respective model with the highest fit.

6.7. As(V) equilibrium sorption capacity correlation with Fe and Mn content

A correlation analysis was performed using obtained sorption data and Fe and Mn content of materials. The analysis was performed using Microsoft Excel Data Analysis toolpack (USA; International). Three different As(V) equilibrium concentrations were chosen – at initial As(V) solution concentration of 300, 100 and 5 mg/L. Correlation coefficients are summarized in **Table 6**. Correlation analysis was performed using all studied materials, as well as separate material groups (where applicable).

Correlation between material's As(V) equilibrium sorption capacity q_e and Fe content is strong (correlation strength ≥0.67 by absolute value) for all groups and for all materials altogether at all studied concentrations.

Correlation between material's As(V) equilibrium sorption capacity q_e and Mn content is strong (correlation strength ≥0.67 by absolute value) only for Ukrainian natural zeolites at initial As(V) solution's concentration of 5 and 100 mg/L. Medium correlation (correlation strength between 0.33 and 0.67 by absolute value) is observed for Ukrainian and Slovakian natural zeolites at initial As(V) solution's concentrations of 300 mg/L. For studied materials altogether at all concentrations and for Slovakian zeolite group at initial As(V) solution's concentration of 5 and 100 mg/L correlation is weak (correlation strength <0.33 by absolute value).

Material	Equilibrium sorption capacity $q_{e,300}$ [mg/g]	Equilibrium sorption capacity $q_{e,100}$ [mg/g]	Equilibrium sorption capacity $q_{e,5}$ [mg/g]	Langmuir monolayer coverage q_m [mg/g]	Improvement [times]	Water remediation [%]
4A	0.15 ± 0.01	0.06 ± 0.00	0.01 ± 0.00	—	—	4.2
Mn-4A	0.39 ± 0.02	0.30 ± 0.02	0.13 ± 0.01	0.40	2.6	43.0
Ukr	0.43 ± 0.02	0.14 ± 0.01	0.02 ± 0.00	—	—	6.6
Fe-Ukr(1)	1.08 ± 0.06	0.96 ± 0.07	0.17 ± 0.02	1.19	2.5	57.2
Fe-Ukr(2)	0.87 ± 0.05	0.40 ± 0.03	0.05 ± 0.01	—	2.0	17.4
Fe-Ukr(3)	0.92 ± 0.05	0.83 ± 0.04	0.24 ± 0.01	0.93	2.1	80.2
Slov	0.36 ± 0.02	0.14 ± 0.01	0.02 ± 0.00	—	—	8.2
Fe-Slov	4.74 ± 0.29	4.08 ± 0.29	0.29 ± 0.03	4.92	13.2	>98.0
Mn-Slov(1)	4.92 ± 0.30	2.21 ± 0.13	0.12 ± 0.01	10.50	13.7	41.2
Mn-Slov(2)	0.66 ± 0.04	0.41 ± 0.02	0.13 ± 0.01	0.71	1.8	44.3
FeMn-Slov	6.96 ± 0.49	3.79 ± 0.27	0.30 ± 0.02	6.82	19.3	>98.0
CaMn-Slov	1.32 ± 0.10	0.51 ± 0.04	0.06 ± 0.00	—	3.7	21.3
KHol	0.24 ± 0.02	0.10 ± 0.01	0.02 ± 0.00	—	—	7.9
Fe-KHol	1.25 ± 0.06	1.18 ± 0.06	0.30 ± 0.02	1.28	5.2	>98.0
13X	0.30 ± 0.02	0.12 ± 0.01	0.01 ± 0.00	—	—	3.2
Fe-13X	1.05 ± 0.05	0.42 ± 0.02	0.08 ± 0.00	—	3.5	26.0

Table 5. As(V) equilibrium sorption capacities.

7. Conclusion

Natural and synthetic zeolites were modified and tailored for As(V) sorption using novel methods. Based on optical microscopy, SEM, EDX and FAAS results, it was proved that zeolites were modified with amorphous Fe(III) oxohydroxide, amorphous Mn(IV) oxide and crystalline mixed oxidation state manganese oxide-chloride $Mn_8O_{10}Cl_3$. FeOOH, and $Mn_8O_{10}Cl_3$-modification improves As(V) sorption capacities of these aluminosilicates. Granulated material with the highest As(V) sorption capacity is $Mn_8O_{10}Cl_3$-FeOOH-modified Slovakian clinoptilolite natural zeolite (6.96 ± 0.49 mg/g). These materials are effective and potential As(V) sorbents, able to remove >98% As(V) in water environments. Sorption capacity of granulated materials (per unit volume) was improved up to 26.5 times. As(V) sorption on FeOOH-modified zeolites follows Langmuir model most precisely, while sorption on unmodified zeolites is described by Freundlich isotherm. In case of $Mn_8O_{10}Cl_3$-modified and MnO_2-modified zeolites, Freundlich and Redlich–Peterson models show the most precise fit, respectively. There is a strong and positive correlation between As(V) sorption capacity and Fe content among all zeolites. Among studied materials, Mn content showed a strong positive correlation only among Ukrainian clinoptilolite natural zeolites.

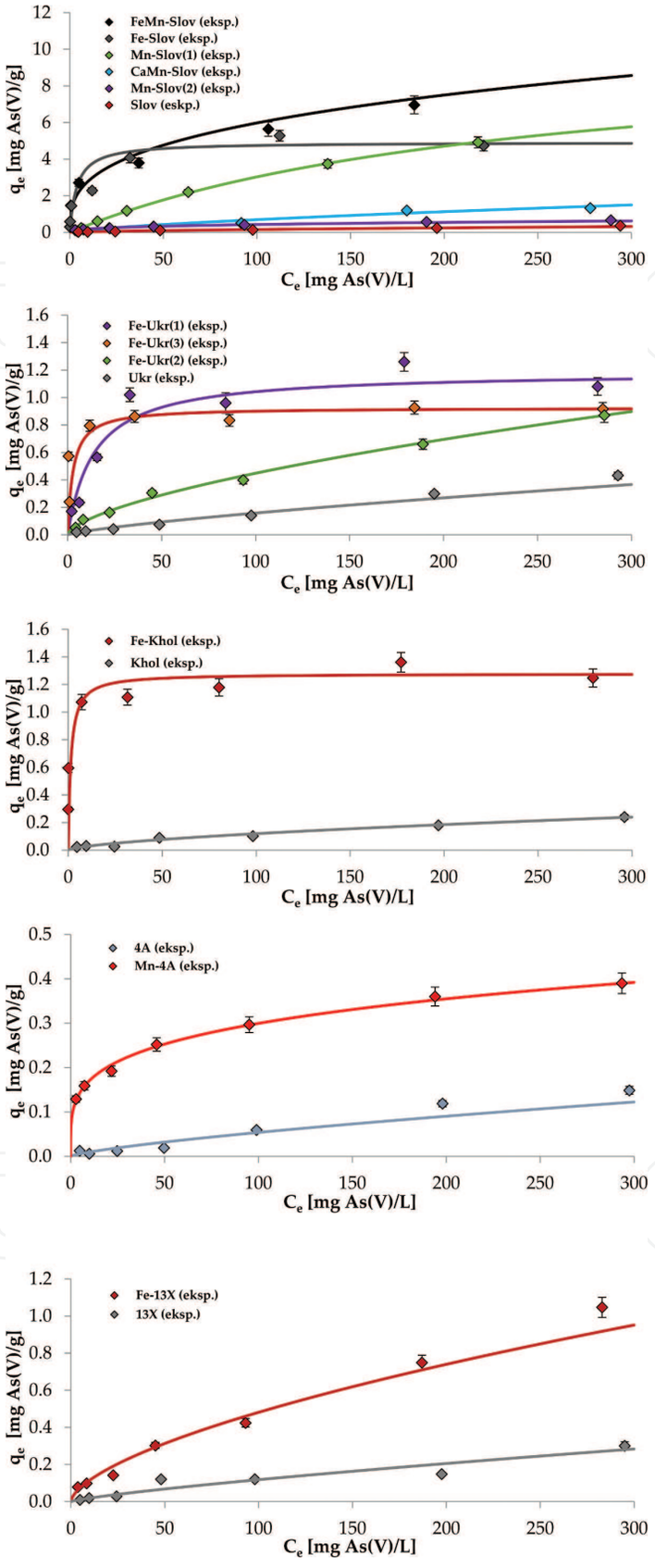

Figure 3. As(V) sorption experimental data and constructed isotherms.

As(V) equilibrium sorption capacity	Correlation with Fe content	Correlation with Mn content
All studied materials		
$q_{e,300}$	0.76	0.20
$q_{e,100}$	0.84	0.17
$q_{e,5}$	0.71	0.05
Ukrainian zeolites		
$q_{e,300}$	0.83	0.50
$q_{e,100}$	0.68	0.70
$q_{e,5}$	0.67	0.94
Slovakian zeolites		
$q_{e,300}$	0.80	0.40
$q_{e,100}$	0.80	0.09
$q_{e,5}$	0.86	−0.07

Table 6. As(V) equilibrium sorption capacities, Fe and Mn content correlation.

Acknowledgements

The author is thankful for an opportunity to perform this work in the laboratory of Department of Environmental Science of Latvian University. This would not be possible without Prof. Maris Klavins, to whom the author is deeply grateful. Acknowledgement also goes to the author's colleagues and teachers who have supported him during this work, Juris Burlakovs, Kristine Rugele and Ruta Ozola.

Author details

Andrey E. Krauklis[1,2,3]*

*Address all correspondence to: andrejs.krauklis@ntnu.no

1 Department of Mechanical and Industrial Engineering, Norwegian University of Science and Technology, Trondheim, Norway

2 Department of Environmental Science, University of Latvia, Riga, LV, Latvia

3 Institute of General Chemical Engineering, Riga Technical University, Riga, LV, Latvia

References

[1] Mukherjee A, Bhattacharya P, Savage K, Foster A, Bundschuh J. Distribution of geogenic arsenic in hydrologic systems: Controls and challenges. Journal of Contaminant Hydrology. 2008;**99**:1-7

[2] Kemper K, Minnatullah K. The World Bank and the Water and Sanitation Programs of South and East Asia, Technical Report No. 31303. 2005

[3] Glocheux Y, Albadarin AB, Mangwandi C, Stewart E, Walker GM. Production of porous aluminium and iron sulphated oxyhydroxides using industrial grade coagulants for optimised arsenic removal from groundwater. Journal of Industrial and Engineering Chemistry. 2014;**25**:56-66

[4] Ma J, Sengupta MK, Yuan D, Dasgupta PK. Speciation and detection of arsenic in aqueous samples: A review of recent progress in non-atomic spectrometric methods. Analytica Chimica Acta. 2014;**831**:1-23

[5] World Health Organization (http://www.who.int/en/)

[6] CAA. Art.1 Res. MS y AS No. 494. Ley 18284, Dec. Reglamentario 2126, Anexo I y II, Marzocchi, Buenos Aires, Argentina. 1994

[7] A textbook of modern toxicology, 3rd edn., ed by Hodgson E. John Wiley and Sons, Hoboken, New Jersey. 2004

[8] Ravenscroft P (http://www.geog.cam.ac.uk/research/projects/arsenic/symposium/S1.2_P_Ravenscroft.pdf)

[9] Bhattacharya P, Claesson M, Bundschuh J, Sracek O, Fagerberg J, Jacks G, Martin RA, Storniolo AR, Thir JM. Distribution and mobility of arsenic in the Río Dulce alluvial aquifers in Santiago del Estero Province, Argentina. Sci Total Environ. 2006;**358**:97-120

[10] Ansone-Bertina L, Klavins M. Sorption of V and VI group metalloids (as, Sb, Te) on modified peat sorbents. Open Chem. 2016;**14**:46-59

[11] Dupont L, Jolly G, Aplincourt M. Arsenic adsorption on lignocellulosic substrate loaded with ferric ion. Environmental Chemistry Letters. 2007;**5**:125-129

[12] Figueiredo H, Quintelas C. Tailored zeolites for the removal of metal oxyanions: Overcoming intrinsic limitations of zeolites. Journal of Hazardous Materials. 2014;**274**:287-299

[13] Zhang F-S, Itoh H. Iron oxide-loaded slag for arsenic removal from aqueous system. Chemosphere. 2005;**60**:319-325

[14] Faure G. Principles and Applications of Inorganic Geochemistry, 2nd Ed., Prentice-Hall. 1998

[15] Bogdanov B, Georgiev D, Angelova K, Yaneva K. International Science Conference. Bulgaria: Stara Zagora; 2009

[16] Hrenovi J, Büyükgüngör H, Orhan Y. Food Technology and Biotechnology. 2003;**41**(2): 157-165

[17] Krauklis A, Ozola R, Burlakovs J, Rugele K, Kirillov K, Trubaca-Boginska A, Rubenis K, Stepanova V, Klavins M. FeOOH and $Mn_8O_{10}Cl_3$ modified zeolites for as(V) removal in aqueous medium. Journal of Chemical Technology and Biotechnology. 2017 Special Issue

[18] Cheung O. Narrow-Pore Zeolites and Zeolite-Like Adsorbents for CO_2 Separation, PhD Thesis, Stockholm University. 2014

[19] Yang RT. Adsorbents: Fundamentals and Applications. Hoboken, New Jersey, USA: John Wiley & Sons, Inc.; 2003

[20] Payne KB, Abdel-Fattah TM. Journal of Environmental Science and Health. 2005;**A40** (4):723-749

[21] Katsoyiannis IA, Zouboulis AI. Removal of arsenic from contaminated water sources by sorption onto iron-oxide-coated polymeric materials. Water Research. 2002;**36**:5141-5155

[22] Sun X, Doner HE. An investigation of arsenate and arsenite bonding structures on goethite by FTIR. Soil Science. 1996;**161**:865-872

[23] Sherman DM, Randall SR. Surface complexation of arsenic(V) to iron(III) (hydr)oxides: Structural mechanism from ab initio molecular geometries and EXAFS spectroscopy. Geochimica et Cosmochimica Acta. 2003;**67**:4223-4230

[24] Мищенко КП, Равдель АА. Краткий справочник физико-химических величин, 7ое Изд., *Л*.: Химия. 1974 (in Russian)

[25] Bundschuh J, Bhattacharya P, Sracek O, Mellano MF, Ramírez AE, del Storniolo AR, Martin RA, Cortés J, Litter MI, Jean JS. Arsenic removal from groundwater of the Chaco-Pampean plain (Argentina) using natural geological materials as adsorbents. Journal of Environmental Science and Health, Part A. 2011;**46**:1297-1310

[26] PubChem Substance and Compound database (https://pubchem.ncbi.nlm.nih.gov PubChem)

[27] Camacho LM, Parra RR, Deng S. Arsenic removal from groundwater by MnO2-modified natural clinoptilolite zeolite: Effects of pH and initial feed concentration. Journal of Hazardous Materials. 2011;**189**:286-293

[28] Manning BA, Fendorf SE, Bostick B, Suarez DL. Environmental Science and Technology. 2002;**36**(5):976-981

[29] Kemmitt RDW, Peacock RD. The Chemistry of Manganese, Technetium and Rhenium: Pergamon Texts in Inorganic Chemistry. Volume I3. Pergamon Press. 1973

[30] Zhang L, Zeng Y, Cheng Z. Journal of Molecular Liquids. 2016;**214**:175-191

[31] Foo KY, Hameed BH. Chemical Engineering Journal. 2010;**156**(1):2-10

[32] Allen SJ, McKay G, Porter JF. Journal of Colloid and Interface Science. 2004;**280**(2):322-333

[33] Dada AO, Olalekan AP, Olatunya AM. Dada O. IOSR Journal of Applied Chemistry. 2012;**3**(1):38-45

[34] F-C W, Liu B-L, K-T W, Tseng R-L. Chemical Engineering Journal. 2010;**162**(1):21-27

[35] http://www.vskpro-zeo.sk/en/zeolite/natural/ Slovakian natural zeolite (acc. 12.04.2016)

[36] http://www.dpzzz.com/ru/info/1/5.html Ukrainian natural zeolite (acc. 27.02.2016)

[37] http://www.zeolite.spb.ru/nat_zeo.htm Russian natural zeolite (acc. 17.05.2016)

[38] Grace Davison – Materials & Packaging Technologies. SYLOSIV Molecular Sieve Powder Brochure (2008)

[39] Ozola R, Krauklis A, Leitietis M, Burlakovs J, Vircava I, Ansone-Bertina L, Bhatnagar A, Klavins M. FeOOH-modified clay sorbents for arsenic removal from aqueous solutions. Environmental. Technology and Innovation. 2016

[40] Jankēvica M, Ansone L, Kļaviņš M. Material Science and Applied Chemistry. 2013;**29**:101-108

[41] Wang S, Gao B, Li Y, Mosa A, Zimmerman AR, Ma LQ, Harris WG, Migliaccio KW. Bioresource Technology. 2015;**181**:13-17

[42] Mahadik KR. Concise Inorganic Pharmaceutical Chemistry. Pragati Books Pvt. Ltd; 2008

[43] http://www.leica-microsystems.com Leica Microscopes (acc. 27.05.2016)

[44] The United States Pharmacopeial Convention. Bulk Density and Tapped Density of Powders, Stage 6 Harmonization. 2011

[45] FMP Group (Australia) Pty. Ltd. Standart Test Method, Bulk Density/Volume Tapped. 2009

[46] World Health Organization. Bulk density and tapped density of powders, Document QAS/11.450 FINAL. 2012